PROCEEDINGS OF SCIENCE

First results on QCD thermodynamics with HISQ action

Alexei Bazavov[*a] **and Peter Petreczky**[b†] **[The HotQCD collaboration]** [‡]
[a]*Department of Physics, University of Arizona, Tucson, AZ 85721, USA*
[b]*Physics Department, Brookhaven National Laboratory, Upton, NY 11973, USA*

We report on investigations of the chiral and deconfinement aspects of the finite temperature transition in 2+1 flavor QCD using the Highly Improved Staggered Quark (HISQ) action on lattices with temporal extent $N_\tau = 6$ and $N_\tau = 8$. We have calculated several physical observables, including the renormalized Polyakov loop, strangeness fluctuations, the renormalized chiral condensate and the chiral susceptibility in the crossover region for physical values of the strange quark mass m_s and light quark masses $m_l = 0.2m_s$ and $0.05m_s$. We compare our findings with previous calculations that use different improved staggered fermion formulations: asqtad, p4 and stout.

The XXVII International Symposium on Lattice Field Theory
July 26-31, 2009
Peking University, Beijing, China

[*]Speaker.

[†]This work has been supported in part by contracts DE-AC02-98CH10886 and DE-FC02-06ER-41439 with the U.S. Department of Energy and contract 0555397 with the National Science Foundation. The numerical calculations have been performed using the USQCD resources at Fermilab as well as the BlueGene/L at the New York Center for Computational Sciences (NYCCS). We thank Z. Fodor and S. Katz for sending us the stout data.

[‡]HotQCD Collaboration members are: A. Bazavov, T. Bhattacharya, M. Cheng, N.H. Christ, C. DeTar, S. Ejiri, S. Gottlieb, R. Gupta, U.M. Heller, K. Huebner, C. Jung, F. Karsch, E. Laermann, L. Levkova, C. Miao, R.D. Mawhinney, P. Petreczky, C. Schmidt, R.A. Soltz, W. Soeldner, R. Sugar, D. Toussaint and P. Vranas

PoS(LAT2009)163

1. Introduction

Improved staggered fermion formulations are widely used to study QCD at non-zero temperatures and densities, see e.g. Ref. [1, 2] for recent reviews. The main reason for this is the fact that they preserve a part of the chiral symmetry of the continuum QCD. This makes the numerical simulations relatively inexpensive because due to absence of an additive mass renormalization the Dirac operator is bounded from below, and also allows one to study the chiral aspects of the finite temperature transition. However, there are at least two problems with staggered fermion formulation. The first one is the validity of the rooting procedure, i.e. the way to reduce the number of tastes from four to one and the other is breaking of the taste symmetry at finite lattice spacing. For the discussion of the validity of rooted staggered fermions see Refs. [3, 4]. To reduce the taste violations smeared links are used in the staggered Dirac operator and different staggered formulations, like p4, asqtad and stout differ in the choice of the smeared gauge links. The smeared gauge links in the p4 and asqtad actions are linear combinations of single links and different staples [5, 6] and therefore are not elements of SU(3) group. It is known that projecting the smeared gauge fields onto the SU(3) group greatly improves the taste symmetry [7]. The stout [8] action and the HISQ action considered here implement the projection of the gauge field onto SU(3) (or simply U(3)) group and thus achieve better taste symmetry at a given lattice spacing. For studying QCD at high temperature it is important to use discretization schemes which improve the quark dispersion relation, thus eliminating the tree level $\mathcal{O}(a^2)$ lattice artifacts in thermodynamic quantities. The p4 and asqtad actions implement this improvement by introducing 3-link terms in the staggered Dirac operator. In this contribution we report on exploratory studies of QCD thermodynamics with the HISQ action which removes tree level $\mathcal{O}(a^2)$ lattice artifacts as well as has projected smeared links that greatly improve the taste symmetry. We also compare our results with previous ones obtained with the asqtad, p4 and stout actions [9, 10, 11, 12, 13].

2. Action and run parameters

The Highly Improved Staggered Quark (HISQ) action developed by the HPQCD/UKQCD collaboration [14] reduces taste symmetry breaking and decreases the splitting between different pion tastes by a factor of about three compared to the asqtad action. The net result, as recent studies show [15], is that a HISQ ensemble at lattice spacing a has scaling violations comparable to ones in an asqtad ensemble at lattice spacing $2/3a$.

In this exploratory study we used the HISQ action in the fermion sector and tree-level Symanzik improved gauge action without the tadpole improvement. The strange quark mass m_s was set to its physical value setting the quantity $\sqrt{2m_K^2 - m_\pi^2} = m_{\eta_{s\bar{s}}} \simeq \sqrt{2Bm_s}$ to the physical value 686.57 MeV. Two sets of ensembles have been generated along the two lines of constant physics (LCP): $m_l = 0.2m_s$ and $m_l = 0.05m_s$. In the first set runs were performed on $16^3 \times 32$ lattices at zero temperature and $16^3 \times 6$ at finite temperature, and in the second set on 32^4 and $32^3 \times 8$ lattices, correspondingly. The parameters and statistics of these runs are summarized in Table 2. The molecular dynamics (MD) trajectories have length of 1 time unit (TU) and the measurements were performed every 5 TUs at zero and 10 TUs at finite temperature. Normally, 300 TUs were discarded for equilibration. The lattice spacing has been determined by measuring the static quark-anti-quark potential and us-

$N_\tau = 6$, $0.2m_s$ LCP runs					$N_\tau = 8$, $0.05m_s$ LCP runs				
β	a, fm	am_s	TU, 0	TU, T	β	a, fm	am_s	TU, 0	TU, T
6.000	0.2297	0.115	3,000	6,000	6.354	0.1578	0.0728	1,095	2,590
6.038	0.2212	0.108	3,000	6,000	6.423	0.1487	0.0670	1,295	2,490
6.100	0.2082	0.100	3,000	6,000	6.488	0.1403	0.0620	1,495	2,690
6.167	0.1954	0.091	3,000	6,000	6.550	0.1326	0.0582	1,395	3,380
6.200	0.1895	0.087	3,000	6,000	6.608	0.1253	0.0542	1,460	3,100
6.227	0.1848	0.084	3,000	6,000	6.664	0.1186	0.0514	1,095	5,000
6.256	0.1800	0.081	3,000	6,000	6.800	0.1047	0.0448	–	2,700
6.285	0.1752	0.079	3,000	6,000	6.950	0.0921	0.0386	–	1.400
6.313	0.1708	0.076	3,000	6,000	7.150	0.0770	0.0320	1,095	1,190
6.341	0.1665	0.074	3,000	6,000					
6.369	0.1622	0.072	3,000	6,000					
6.396	0.1582	0.070	3,000	6,000					
6.450	0.1505	0.068	3,000	6,000					

Table 1: The parameters of the numerical simulations: gauge coupling, strange quark mass and the number of time units (TU), i.e. the number of MD trajectories for each run. Here TU, 0 stands for the number of time units for zero-temperature runs, while TU, T is the number of time units for finite-temperature runs.

	$0.2m_s$ LCP	$0.05m_s$ LCP
m_π	306-312	156-161
m_K	522-532	493-501
m_ρ	850-883	760-808
m_N	1130-1183	1014-1083

Table 2: Ranges of masses (in MeV) of several hadrons for the two sets of ensembles.

ing the Sommer scale $r_0 = 0.469$ fm. The masses of several hadrons measured on zero-temperature ensembles fall into ranges summarized in Table 2.

As mentioned above the lattice artifacts for the HISQ action are significantly reduced compared to the asqtad action. The taste violations are strongest in the pseudo-scalar meson sector. Therefore we studied the splitting of pseudo-scalar meson masses in the 8 different multiplets. The results are shown in Fig. 1 and compared to the stout results. The splittings are 2 to 3 times smaller than in the calculations with the asqtad action and also somewhat smaller than for the stout action. The smaller taste violations also result in better scaling of other hadron masses. In Fig. 1 we also show the kaon, rho-meson and nucleon masses. As one can see for the small, almost physical, value of the light quark mass we get reasonable agreement between the lattice results and the experimental values.

3. Deconfinement transition

The deconfinement transition is usually studied using the renormalized Polyakov loop [12, 16,

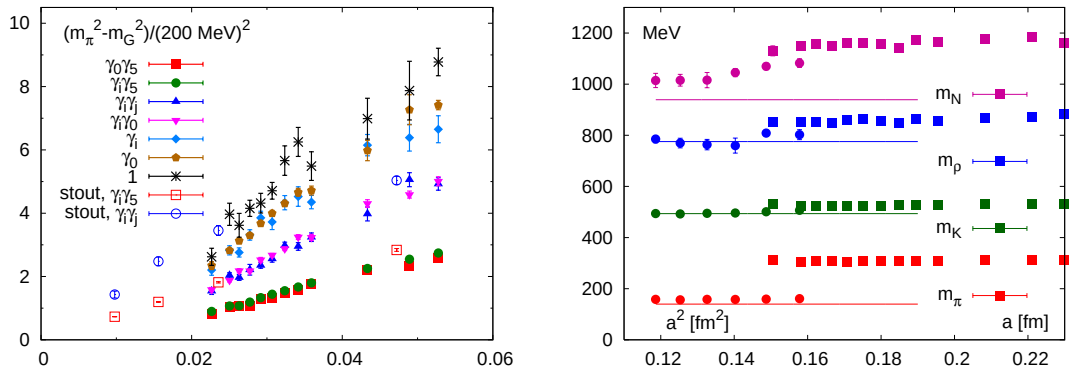

Figure 1: The splitting between different pion multiplets (left) and hadron masses (right) calculated for the HISQ action. In the right panel squares indicate ensembles along the $0.2m_s$ LCP, and circles along the $0.05m_s$ LCP.

17, 18]. It is related to the free energy of a static quark anti-quark pair at infinite separation $F_\infty(T)$

$$L_{ren}(T) = \exp(-F_\infty(T)/(2T)), \tag{3.1}$$

obtained from the bare Polyakov loop as

$$L_{ren}(T) = z(\beta)^{N_\tau} L_{bare}(\beta) = z(\beta)^{N_\tau} \left\langle \frac{1}{3}\mathrm{Tr} \prod_{x_0=0}^{N_\tau-1} U_0(x_0,\vec{x}) \right\rangle . \tag{3.2}$$

Here the multiplicative renormalization constant $z(\beta)$ is related to the additive normalization of the potential $c(\beta)$ as $z(\beta) = \exp(-c(\beta)/2)$. To make the comparison with the stout results easy here we chose the normalization constant $c(\beta)$ such that the potential is zero at distance $r = r_0$. This choice is different from the one used in Refs. [17, 18]. Our results for the quark mass $m_q = 0.05m_s$ on $32^3 \times 8$ lattices are shown in Fig. 2 and compared to the stout and p4 calculations. As one can see the HISQ calculations agree reasonably well with the stout results if the scale is set by r_0 in the stout calculations [1]. On the other hand, the renormalized Polyakov loop calculated with the p4 action is considerably smaller at low temperatures. At temperatures $T > 200$ MeV we see good agreement for different actions. The fluctuation of strangeness is also a good indicator for the deconfinement transition. It can be defined as the second derivative of the free energy density with respect to the strange quark chemical potential

$$\frac{\chi_s(T)}{T^2} = \frac{1}{T^3 V} \frac{\partial^2 \ln Z(T,\mu_s)}{\partial(\mu_s/T)^2}\bigg|_{\mu_s=0} . \tag{3.3}$$

At low temperatures strangeness is carried by massive hadrons and therefore strangeness fluctuations are suppressed. At high temperatures strangeness is carried by quarks and the effect of the non-zero strange quark mass is small. Therefore, in the transition region the strangeness fluctuation rises and eventually reaches a value close to that of an ideal quark gas. Our numerical results for

[1] In what follows we will show the stout results using the temperature scale set by r_0 instead of the kaon decay constant f_K. We used the published values of r_0 and f_K in Refs. [12, 13] to convert the two scales.

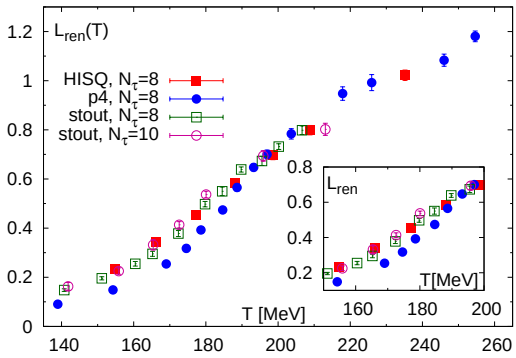

Figure 2: The renormalized Polyakov loop as function of the temperature calculated for the HISQ, stout and p4 actions at the physical value of light quark masses.

strangeness fluctuations are shown in Fig. 3 for two values of the light quark masses, $m_q = 0.05m_s$ and $0.2m_s$. In the case of the heavier quark mass we compare our results with the ones obtained with the asqtad action for $m_q = 0.2m_s$. As one can see the strangeness fluctuations are larger for the HISQ action at low temperatures, $T < 210$ MeV. In other words, the transition region in the HISQ calculation shifts toward smaller temperatures. This behavior is in fact expected. Due to smaller taste symmetry violation pseudo-scalar masses as well as other hadron masses are smaller and therefore strangeness fluctuations are larger. For the smaller (physical) quark mass we compare our calculations with the results obtained using the p4 action [10, 11] and the stout action [12, 13]. At low temperatures, $T < 200$ MeV the HISQ results are significantly larger than the p4 results but are in good agreement with the stout results. At high temperatures, $T > 200$ MeV the strangeness fluctuations calculated with the HISQ action are in reasonable agreement with the p4 results as well as the $N_\tau = 12$ stout results. We also see that in this temperature region the stout results show some cutoff (N_τ) dependence. This is due to the fact that the tree level $\mathcal{O}(a^2)$ lattice artifacts are not removed in the stout action. In the low temperature region we expect that the Hadron Resonance Gas (HRG) model gives a reasonably good description of the thermodynamic quantities, including strangeness fluctuations. Therefore in Fig. 3 we show the prediction of the HRG model. As one can see the lattice results fall below the HRG model results. The discrepancy between the HRG model and the lattice data becomes larger at smaller temperatures, although the model is expected to be more reliable at smaller temperatures. This is presumably due to taste violation, especially in the pseudo-scalar meson sector. Due to non-negligible splitting in the pseudo-scalar meson mass the contribution of kaons to strangeness fluctuations appears to be smaller than expected in the continuum.

4. The chiral transition

In the limit of zero light quark masses QCD has a chiral symmetry and the finite temperature transition is a true phase transition. The order parameter for this transition is the light chiral condensate $\langle \psi\bar{\psi}\rangle_l$. However, even at finite values of the quark mass the chiral condensate will show a rapid change in the transition region indicating an effective restoration of the chiral symmetry.

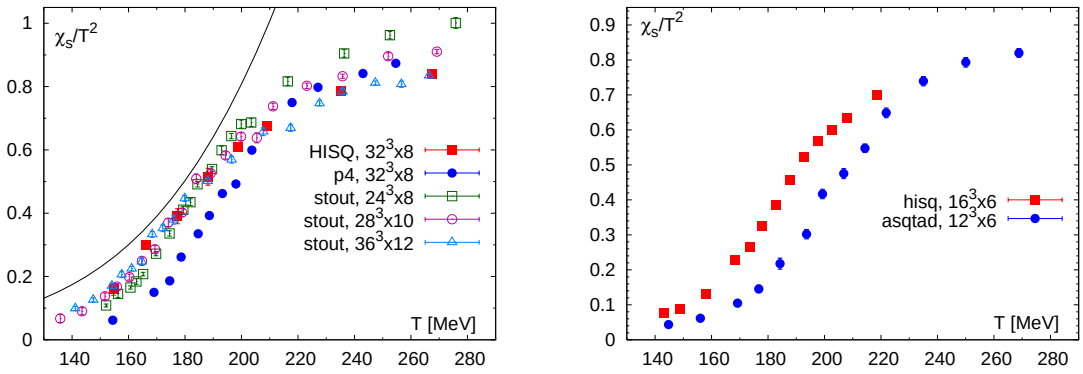

Figure 3: The strangeness fluctuations $\chi_s(T)$ calculated for $m_q = 0.05m_s$ (left) and $m_q = 0.2m_s$ (right). For the physical quark mass $m_q = 0.05m_s$ we compare our results with previous calculations performed with the stout and p4 actions. The solid line in the left plot shows the prediction of the HRG model.

Since the chiral condensate has an additive ultraviolet renormalization we consider the subtracted chiral condensate [17, 18]

$$\Delta_{l,s}(T) = \frac{\langle\bar{\psi}\psi\rangle_{l,\tau} - \frac{m_l}{m_s}\langle\bar{\psi}\psi\rangle_{s,\tau}}{\langle\bar{\psi}\psi\rangle_{l,0} - \frac{m_l}{m_s}\langle\bar{\psi}\psi\rangle_{s,0}}. \tag{4.1}$$

Here the subscripts l and s refer to light and strange quark condensates respectively, while the subscripts 0 and τ refer to the zero and finite temperature cases. In Fig. 4 we show the renormalized chiral condensate calculated with the HISQ action and compare it with results obtained with the stout action [13] as well as with the p4 results [10, 11]. Our results agree resonably well with the $N_\tau = 8$ stout results and the agreement between the HISQ and stout results is even better if one considers $N_\tau = 10$ and $N_\tau = 12$. On the other hand, the subtracted chiral condensate is considerably smaller than for the p4 action. This is presumably due to the larger taste violating effects in the p4 case. We also considered the fluctuations of the chiral condensate, which is just the disconnected part of the chiral susceptibility χ_{disc}. The corresponding results are shown in Fig. 4. For true phase transition the chiral susceptibility should show a peak at the critical temperature. The numerical results indeed show some peak-like structure. However, as discussed in Ref. [19] it is not easy to differentiate between the increase in the chiral condensate due to nearby critical point and the effect of the Goldstone modes. Certainly, much more detailed studies are needed here.

5. Conclusions

In this contribution we discussed first results on QCD thermodynamics with the HISQ action. The use of this action allows one to minimize cutoff effects in thermodynamic quantities due to lattice artifacts in the quark dispersion relation and taste symmerty breaking. In fact, the HISQ action gives the smallest taste violation in the pseudo-scalar meson sector if measured though the mass splittings. We have calculated the renormalized Polyakov loop, the chiral condensate and the strangeness fluctuations on $N_\tau = 6$ and $N_\tau = 8$ lattices. We find good agreement between our results and the ones obtained with the stout action in the low temperature region, $T < 200$ MeV. At the same time present results disagree with the p4 results. In the high temperature region, where

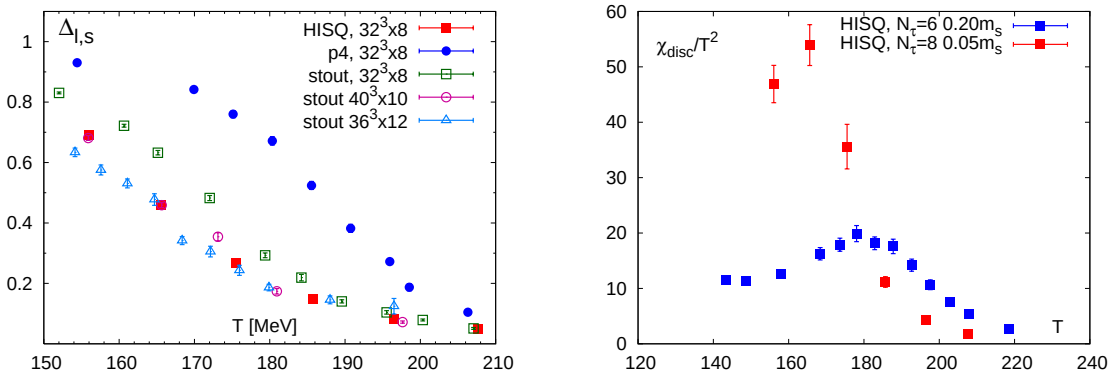

Figure 4: The subtracted chiral condensate (left) and the disconnected part of the chiral susceptibility (right). For the subtracted chiral condensate we also compare our results with calculations performed for stout and p4 actions. Note that in the right panel we show the disconnected chiral susceptibility for the HISQ action for two LCPs: $0.2m_s$ and $0.05m_s$.

there are visible cutoff effects in the stout calculations the HISQ results agree resonably well with the p4 results as well as with the stout results obtained on $N_\tau = 12$.

References

[1] C. E. DeTar, PoS **LATTICE2008**, 001 (2008)

[2] P. Petreczky, arXiv:0908.1917 [hep-ph].

[3] S. R. Sharpe, PoS **LAT2006**, 022 (2006)

[4] M. Creutz, PoS **LAT2007**, 007 (2007)

[5] F. Karsch, E. Laermann and A. Peikert, Nucl. Phys. B **605**, 579 (2001)

[6] K. Orginos, D. Toussaint and R. L. Sugar [MILC Collaboration], Phys. Rev. D **60**, 054503 (1999)

[7] A. Hasenfratz, Nucl. Phys. Proc. Suppl. **119**, 131 (2003)

[8] Y. Aoki, Z. Fodor, S. D. Katz and K. K. Szabo, JHEP **0601**, 089 (2006)

[9] C. Bernard *et al.* [MILC Collaboration], Phys. Rev. D **71**, 034504 (2005)

[10] M. Cheng et. al. (RBC-Bielefeld Coll.), arXiV:0911.2215

[11] P. Petreczky, these proceedings

[12] Y. Aoki, Z. Fodor, S. D. Katz and K. K. Szabo, Phys. Lett. B **643**, 46 (2006)

[13] Y. Aoki, S. Borsanyi, S. Durr, Z. Fodor, S. D. Katz, S. Krieg and K. K. Szabo, JHEP **0906**, 088 (2009)

[14] E. Follana *et al.* [HPQCD collaboration and UKQCD collaboration], Phys. Rev. D **75** (2007) 054502

[15] A. Bazavov *et al.* [MILC Collaboration], PoS **LAT2009**, 123 (2009)

[16] O. Kaczmarek, F. Karsch, P. Petreczky and F. Zantow, Phys. Lett. B **543**, 41 (2002)

[17] M. Cheng *et al.*, Phys. Rev. D **77**, 014511 (2008)

[18] A. Bazavov *et al.*, Phys. Rev. D **80**, 014504 (2009)

[19] S. Ejiri *et al.*, arXiv:0909.5122 [hep-lat].